Supplementary Information (SI) for Materials Chemistry Frontiers.
This journal is © the Partner Organisations 2026

Supplementary Information

Commercial-grade zeolite A synthesis from natural stellerite and clinoptilolite for exceptional Sr^{2+} removal performance

Haoyang Zhang[a, †], Binyu Wang[b, †], Yida Zhou[c], Junyao Pan[a], Shuang Liu[a], Changchang Fan[a], Pan Xu[a], Junhui Guo[d], Shaozhong Peng[d, *], Wenfu Yan[a, *]

[a] *State Key Laboratory of Inorganic Synthesis and Preparative Chemistry, College of Chemistry, Jilin University, Changchun 130012, P. R. China*

[b] *Changchun Institute of Optics, Fine Mechanics and Physics, Chinese Academy of Sciences, 130033 Changchun, Jilin, China; State Key Laboratory of Advanced Manufacturing for Optical Systems, 130033 Changchun, Jilin, China; University of Chinese Academy of Sciences, University of Chinese Academy of Sciences, 100049 Beijing, China*

[c] *National Engineering Research Center of Lower-Carbon Catalysis Technology, State Key Laboratory of Catalysis, Dalian Institute of Chemical Physics, Chinese Academy of Sciences, Dalian 116023, P. R. China*

[d] *SINOPEC (Dalian) Research Institute of Petroleum and Petrochemicals Co., Ltd., Dalian 116045, P. R. China*

† These authors contributed equally.

***Corresponding authors:**

E-mail: pengshaozhong.fshy@sinopec.com (Shaozhong Peng), yanw@jlu.edu.cn (Wenfu Yan).

1. Methods and characterization

1.1. Static water adsorption for zeolites A

The static water adsorption was carried out at 25°C with the following procedure, described in GB 6287–86: 1.5 g of zeolite A was heated at 550°C for 1 h and quickly transferred into a dry bottle with a mass of m_1. Subsequently, the open bottle was transferred into a vacuum dryer. Once the pressure in the dryer was less than 1.0×10^3 Pa, the bottle was taken out and weighed immediately as m_2. Finally, the bottle was transferred into a desiccator filled with saturated NaCl aqueous solution and kept for 24 h at 25°C. The weight of the bottle was recorded as m_3. The static water adsorption capacity was calculated according to the following equation:

$$X\ (\%) = \frac{m_3 - m_2}{m_2 - m_1} \times 100\#(1)$$

1.2. Sr^{2+} removal

Batch experiments were conducted to evaluate the removal performance of HEU-LTA, STI-LTA and commercial 4A for Sr^{2+} removal at temperatures of 25°C, 60°C, and 80°C. Typically, 10 mg of the synthesized zeolite A was dispersed in 10 mL of solution with varying Sr^{2+} concentrations. The initial pH of the solution was adjusted using 1.0 M NaOH or 1.0 M HCl, and the solution was stirred for 8 h. The water content physically adsorbed in powder zeolite A was determined by thermogravimetric analysis (TGA), and subsequent calculations of adsorption capacity were based on the mass of the "dry" zeolite. The solid and liquid phases were separated using a 0.22 μm nylon membrane filter. The concentrations of Sr^{2+} in the liquid phase were measured using inductively coupled plasma optical emission spectrometry (ICP-OES). The removal efficiency (R), equilibrium adsorption capacity (Q_e, $mg \cdot g^{-1}$), and distribution coefficient (K_d, $mL \cdot g^{-1}$) were calculated using the following equations:

$$R\ (\%) = \frac{C_i - C_e}{C_i} \times 100\ ,\#(2)$$

$$Q_e = \frac{(C_i - C_e) \times V}{m}, \#(3)$$

and

$$K_d = {Q_e}/{C_e}, \#(4)$$

where C_i and C_e are the initial and the equilibrium concentrations (mg·L^{-1}) of Sr^{2+} in solution, V is the solution volume (L), and m is the mass of the "dry" zeolite (g). Commercial 4A was used as a reference in batch experiments.

1.2.1. Influence of the solid-to-liquid ratio

The effect of the solid-to-liquid ratio on Sr^{2+} removal was evaluated by varying the ratio (g/mL) as 1/200, 1/500, 1/1000, 1/2000, and 1/5000. The initial concentration of Sr^{2+} was set at 100 mg·L^{-1}, with the initial pH adjusted to 6. The contact time for the experiments was maintained at 8 h.

1.2.2. Influence of initial pH

To assess the impact of initial pH on Sr^{2+} removal, the pH was adjusted in the range of 2 to 13 using 1.0 M NaOH or 1.0 M HCl solutions. A solid-to-liquid ratio of 1/1000 was used. The initial concentration of Sr^{2+} was maintained at 100 mg·L^{-1}, with a contact time of 8 h.

1.2.3. Selectivity

The selectivity of HEU-LTA and STI-LTA in removing Sr^{2+} was investigated using solutions with an initial concentration of 5 mg·L^{-1} of Sr^{2+}. The solutions also contained competing ions (Na^+, K^+, Ca^{2+}, or Mg^{2+}) at molar ratios of $M^{+/2+}/Sr^{2+}$ of 0, 100/1, or 1000/1. In the competitive ion experiments, the cations of Na^+, K^+, Ca^{2+} and Mg^{2+}, were mixed at a molar ratio of 1: 1: 1: 1. The solid-to-liquid ratio for Sr^{2+} removal was 1/1000. The initial pH was set at 6, with a contact time of 8 h.

1.2.4. Adsorption kinetics

The influence of contact time on Sr^{2+} removal was studied by varying the contact time from 5 min to 600 min at pre-determined intervals. The solid-to-liquid ratio for Sr^{2+} removal was set at 1/1000. The initial concentration of Sr^{2+} was maintained at 100 $mg \cdot L^{-1}$, with the initial pH set at 6. The experimental data were fitted to the pseudo-first-order and pseudo-second-order kinetic models, described by the following equations:

Pseudo-first-order model:[1]

$$Q_t = Q_e\left(1 - e^{-K_1 t}\right), \#(5)$$

where Q_e is the equilibrium adsorption capacity ($mg \cdot g^{-1}$), Q_t is the adsorption amount ($mg \cdot g^{-1}$) at time t (min), and K_1 is the rate constant of the pseudo-first-order kinetic equation (min^{-1}).

Pseudo-second-order model:[2, 3]

$$Q_t = \frac{K_2 Q_e^2 t}{1 + K_2 Q_e t}, \#(6)$$

where K_2 is the rate constant of the pseudo-second-order kinetic equation ($g \cdot mg^{-1} \cdot min^{-1}$), and other variables are as defined above.

1.2.5. Adsorption isotherms

The adsorption isotherms of Sr^{2+} were studied to evaluate the effects of initial concentration and temperature. Experiments were conducted at 25°C, 60°C, and 80°C, with initial concentrations of Sr^{2+} ranging from 50 $mg \cdot L^{-1}$ to 400 $mg \cdot L^{-1}$. The solid-to-liquid ratio for Sr^{2+} removal was 1/1000. The initial pH was set at 6, with a contact time of 8 h. Two models were used to describe the adsorption isotherms:

Langmuir model:[4]

$$Q_e = \frac{Q_m K_L C_e}{1 + K_L C_e}, \#(7)$$

where Q_m is the maximum adsorption capacity ($mg \cdot g^{-1}$), and K_L is a constant related to adsorption energy ($L \cdot mg^{-1}$).

Freundlich model:[5]

$$Q_e = K_F C_e^{\frac{1}{n}}, \#(8)$$

where Q_e is the equilibrium adsorption capacity ($mg \cdot g^{-1}$), C_e is the equilibrium concentration of the adsorbate ($mg \cdot L^{-1}$), K_F and n represent the adsorption capacity at specific concentration ($mg^{1-1/n} \cdot L^{1/n} \cdot g^{-1}$) and strength, respectively. The fitting of Langmuir and Freundlich isotherm models to experimental data was conducted with linear regression.

1.2.6. Reusability

The reusability of HEU-LTA, STI-LTA and commercial 4A in removing Sr^{2+} was studied. The solid-to-liquid ratio for Sr^{2+} removal for both zeolite A was 1/1000. The initial pH was set at 6, with a contact time of 8 h. After each adsorption cycle, HEU-LTA, STI-LTA and commercial 4A were regenerated by immersion in 1 M NaCl solution for 12 h, followed by thorough washing with deionized water. The adsorption-regeneration cycle was repeated 4 times.

1.3. Characterization

Powder X-ray Diffraction (PXRD): PXRD patterns were collected in the 2θ range of 4-40° using a Rigaku D/Max 2550 diffractometer with Cu Kα radiation (λ = 1.5418 Å) and an angular step size of 0.02°. Relative crystallinity of HEU-LTA and STI-LTA was calculated as:

$$R = \frac{\sum A(characteristic\ peaks)}{\sum A(characteristic\ peaks\ of\ reference\ sample)} \times 100\ \%, \#(9)$$

where R is the relative crystallinity, A is the peak area of a characteristic peak.

X-ray Fluorescence (XRF): The chemical composition of natural clinoptilolite, natural stellerite, HEU-LTA, and STI-LTA was determined using a PANalytical, AXIOS XRF spectrometer.

Scanning Electron Microscopy (SEM) and Energy Dispersive Spectrometer (EDS): The morphology of natural clinoptilolite, natural stellerite, their activated

products, HEU-LTA and STI-LTA, and EDS-point analysis for chemical composition analysis of HEU-LTA and STI-LTA were analyzed using a Jeol JSM-7800F SEM.

High Resolution Transmission Electron Microscopy (HRTEM): The morphology of HEU-LTA and STI-LTA was studied using a Talos F200S G2 HRTEM.

Thermogravimetric Analysis (TGA): TGA was conducted in air using a TGA Q500 analyzer, with a heating rate of 10°C·min^{-1} from ambient temperature to 800°C.

Inductively Coupled Plasma Optical Emission Spectrometer (ICP-OES): The concentration of Sr^{2+} in solution was measured using a Thermo Scientific iCAP 7600 DUO ICP-OES.

Solid-state Magic Angle Spinning Nuclear Magnetic Resonance (MAS NMR): The local environments of atoms for natural clinoptilolite, natural stellerite, their activated products, HEU-LTA and STI-LTA and the products with various crystallization times in the induction period were examined through ^{27}Al and ^{29}Si solid-state MAS NMR measurements on a Bruker Avance NEO system with a 14.09 T magnetic field.

Nitrogen Adsorption/ Desorption Isotherms: Measured at 77 K using a BSD-660M analyzer, after degassing samples at 573 K for at least 8 h. Textural properties, including total surface area, external surface area, and micropore volume, were measured using the Brunauer-Emmett-Teller (BET) equation and *t*-plot method, respectively. The total pore volume was obtained from the amount of N_2 adsorbed at $P/P_0 = 0.99$.

Ultraviolet Raman resonance (UV-Raman): UV-Raman spectra were recorded on a HS325 Raman spectrometer using the 325 nm light source.

Fourier Transform Infrared (FT-IR): FT-IR spectra were recorded between 400 to 4000 cm^{-1} by using Bruker VERTEXV 80 V spectrometer.

2. Figures and tables

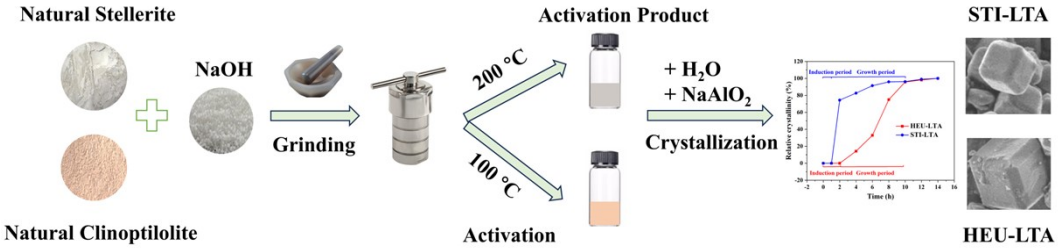

Scheme S1 Schematic illustration of the synthesis of zeolite A using natural clinoptilolite or natural stellerite as raw materials.

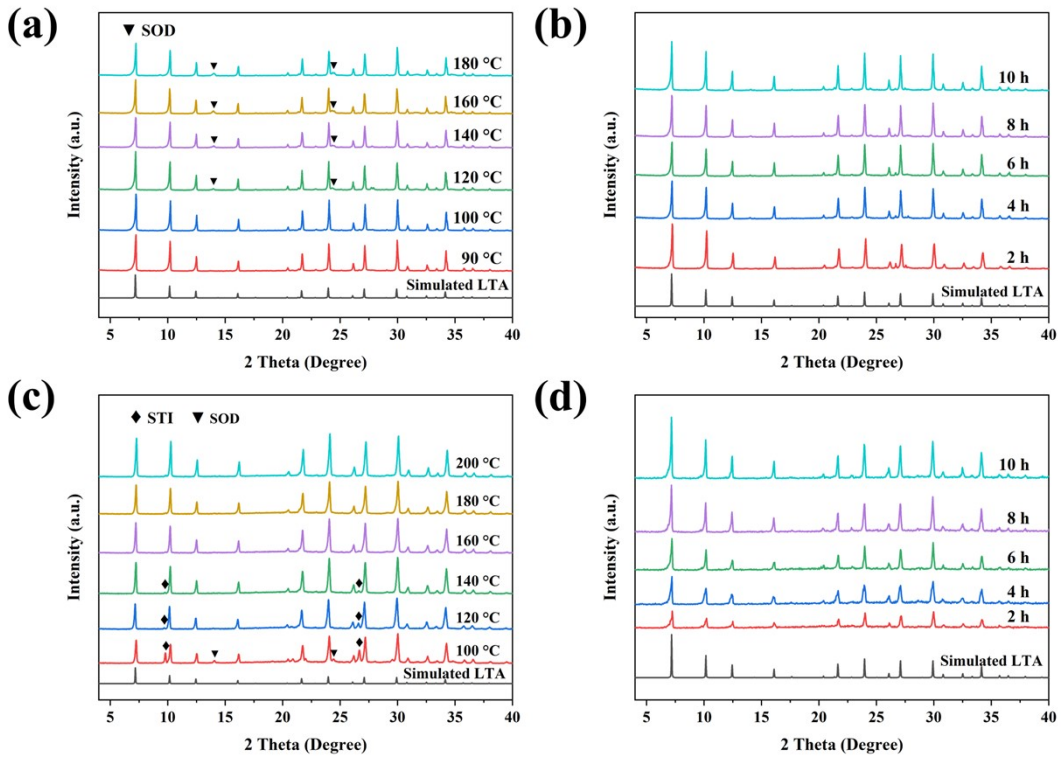

Fig. S1 XRD patterns of HEU-LTA synthesized with various activated temperatures (a) and activated time (b); XRD patterns of STI-LTA synthesized with various activated temperatures (c) and activated time (d).

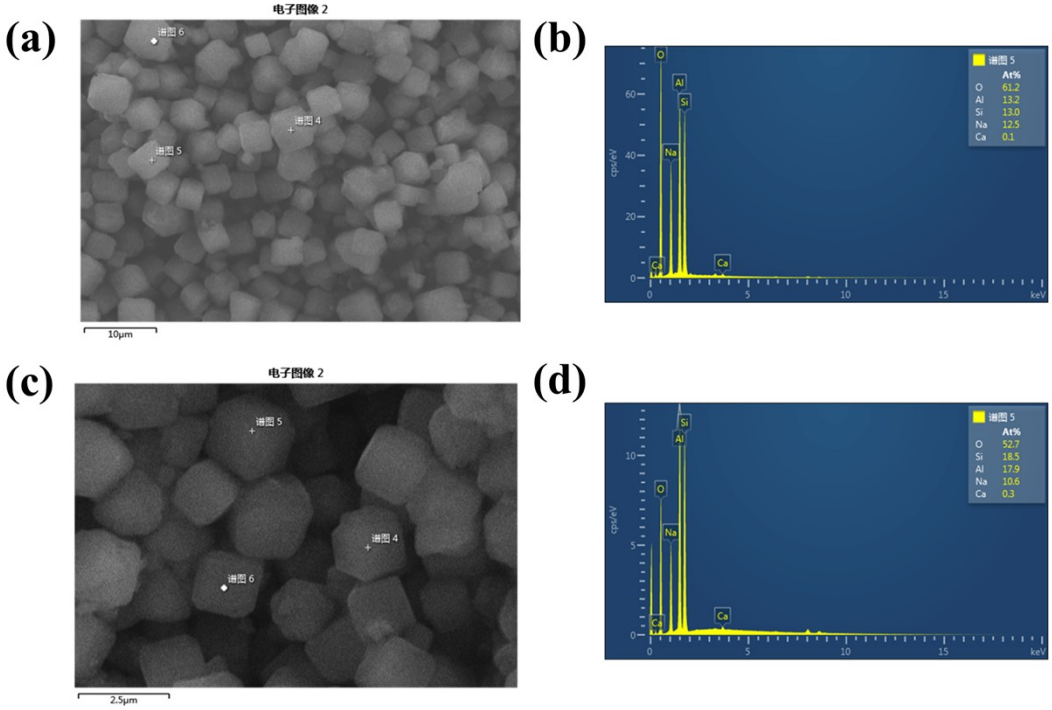

Fig. S2 The SEM-EDS images and elemental composition of HEU-LTA(a) (b) and STI-LTA (c) (d).

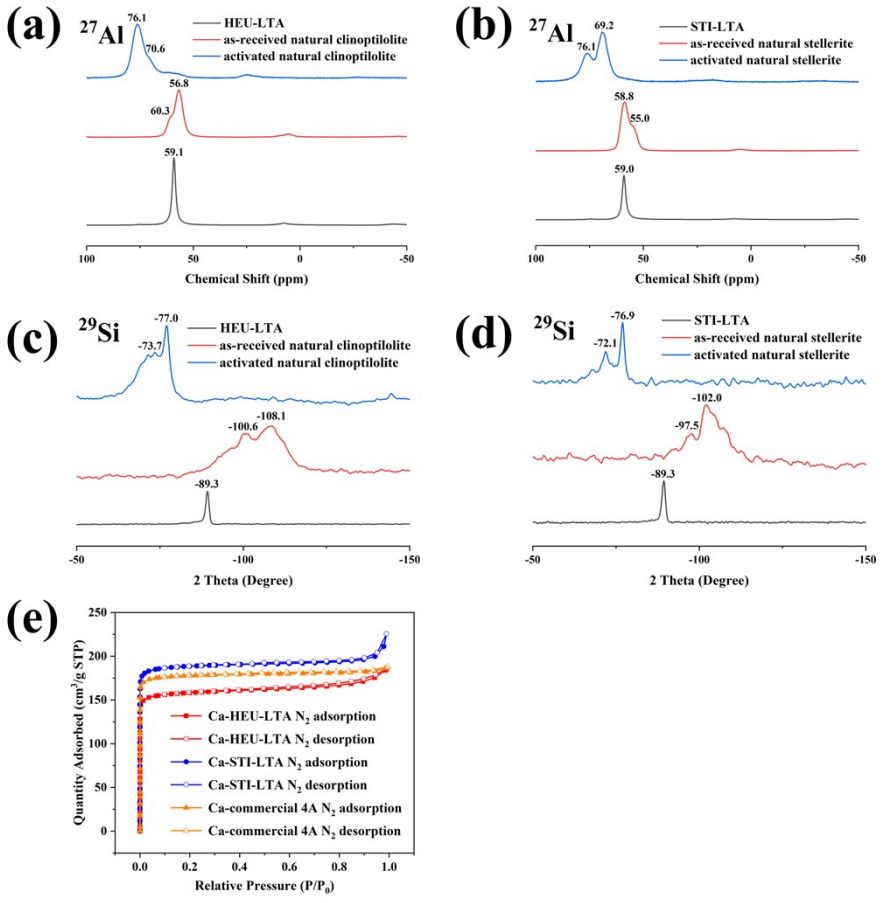

Fig. S3 ^{27}Al MAS NMR spectra of (a) HEU-LTA, natural clinoptilolite, and the corresponding activated product; (b) STI-LTA, natural stellerite, and the corresponding activated product; ^{29}Si MAS NMR spectra of (c) HEU-LTA, natural clinoptilolite, and the corresponding activated product; (d) STI-LTA, natural stellerite, and the corresponding activated product; (e) N_2 adsorption–desorption isotherms of HEU-LTA and STI-LTA after Ca^{2+} ion exchange.

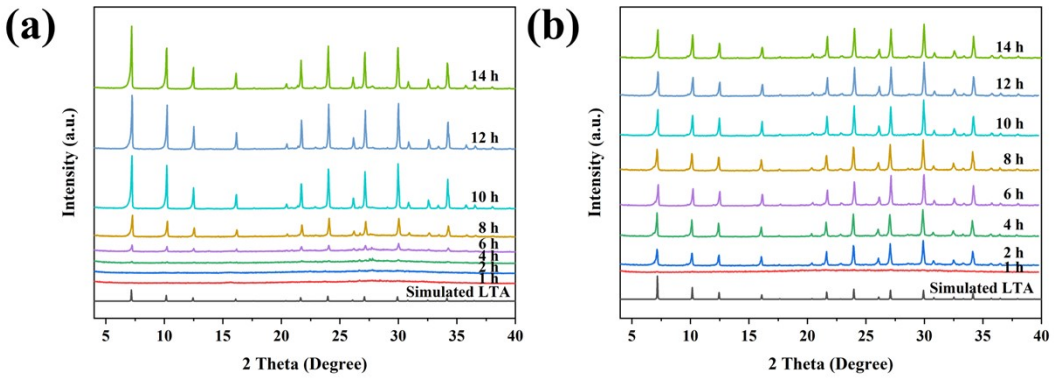

Fig. S4 The XRD patterns of HEU-LTA (a) and STI-LTA (b) isolated throughout the hydrothermal treatment period.

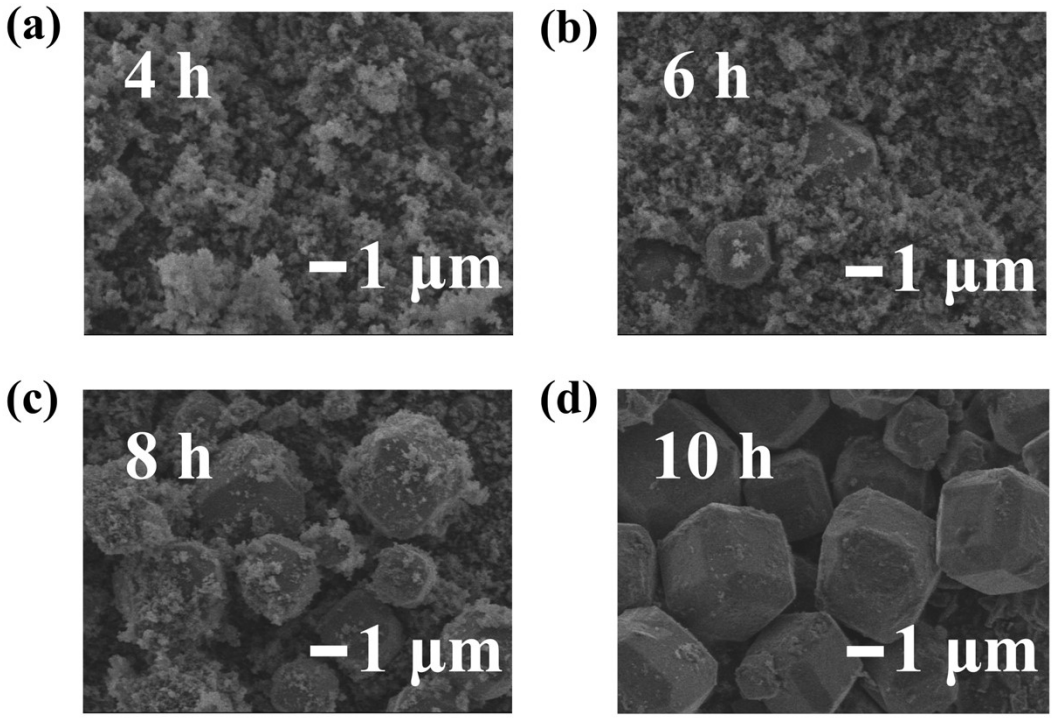

Fig. S5 SEM images of HEU-LTA with various crystallization times.

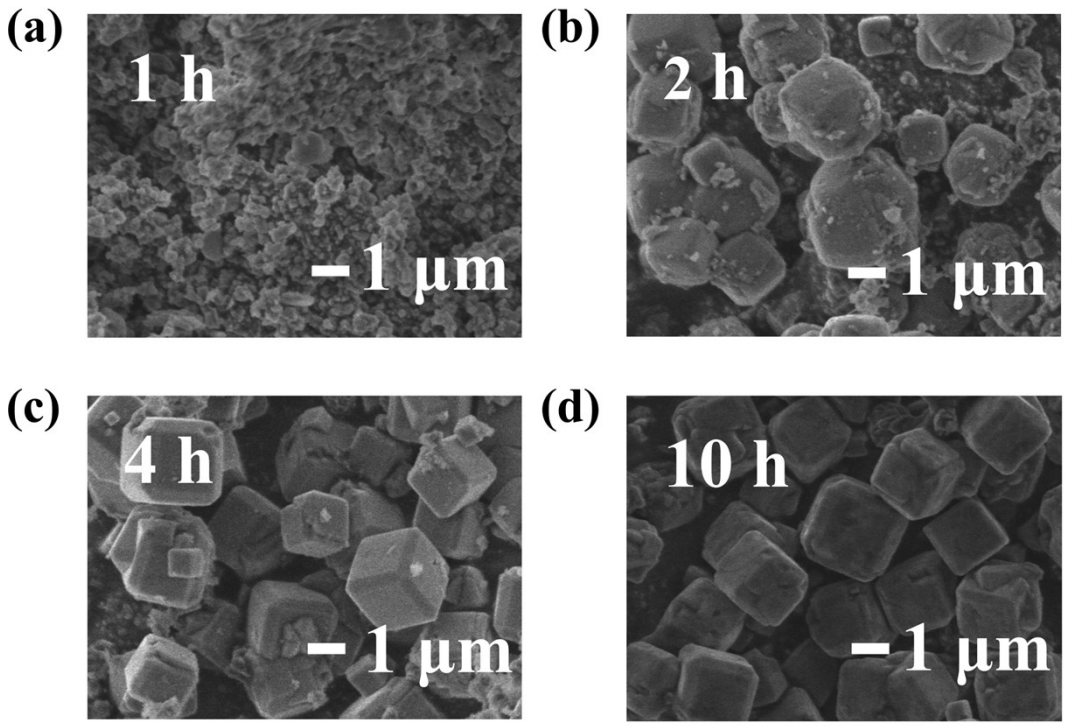

Fig. S6 SEM images of STI-LTA with various crystallization times.

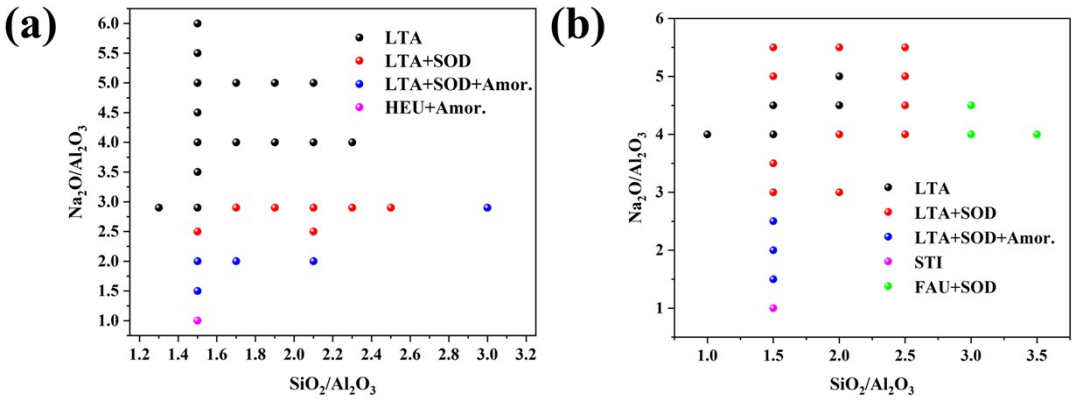

Fig. S7 Crystallization fields of HEU-LTA (a) and STI-LTA (b) as a function of gel composition and crystallization temperature.

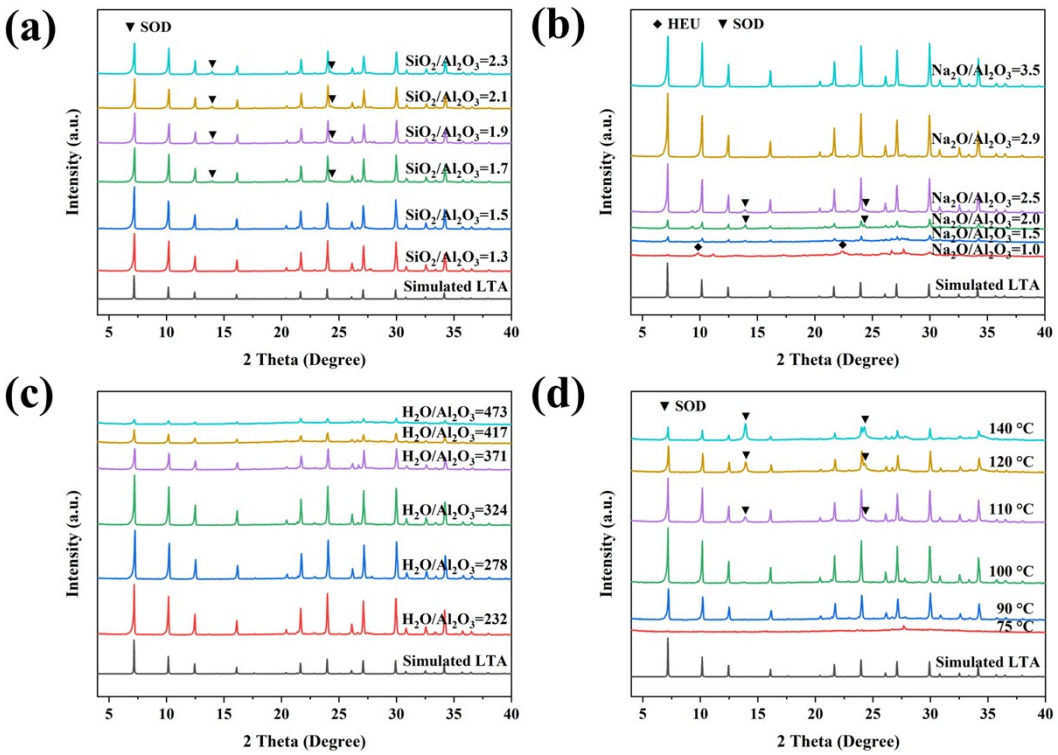

Fig. S8 XRD patterns of HEU-LTA synthesized from the initial gel with various Na_2O/Al_2O_3 ratios (a), SiO_2/Al_2O_3 ratios (b), H_2O/Al_2O_3 ratios (c), and various crystallization temperatures (d).

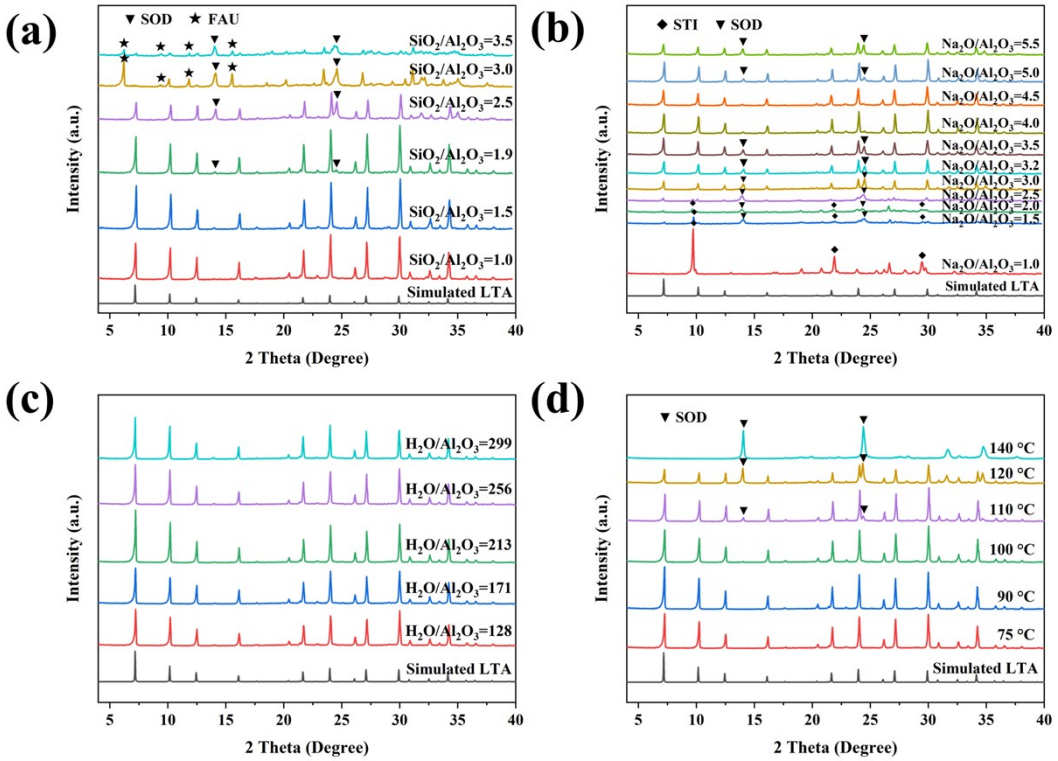

Fig. S9 XRD patterns of STI-LTA synthesized from the initial gel with various

Na_2O/Al_2O_3 ratios (a), SiO_2/Al_2O_3 ratios (b), H_2O/Al_2O_3 ratios (c), and various crystallization temperatures (d).

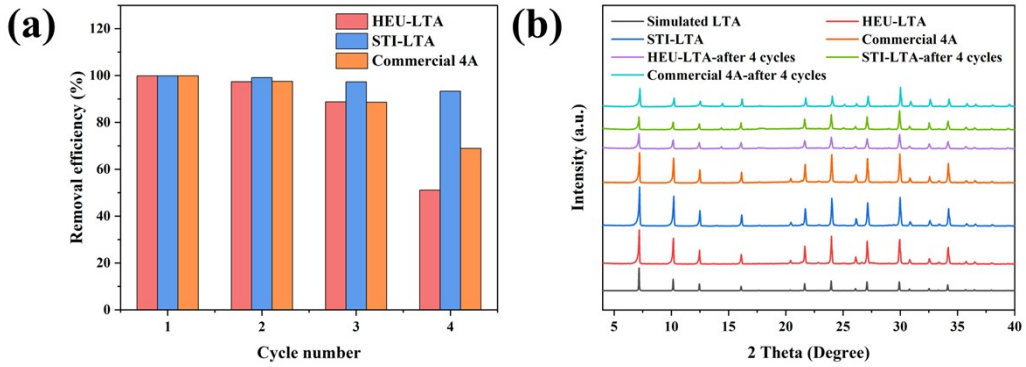

Fig. S10 Reusability performance of HEU-LTA, STI-LTA, and commercial 4A for Sr^{2+} removal over multiple adsorption–desorption cycles (a); XRD patterns of fresh adsorbents and adsorbents after four cycles (b).

Table S1 Composition of natural clinoptilolite (as-received), natural stellerite (as-received), HEU-LTA and STI-LTA determined by XRF.

Component	Wt.% of natural clinoptilolite (as-received)	Wt.% of natural stellerite (as-received)	Wt.% of HEU-LTA	Wt.% of STI-LTA
SiO_2	76.3	63.8	39.2	39.8
Al_2O_3	14.1	15.8	34.6	36.6
Na_2O	0.5	0.3	20.6	21.6
CaO	2.9	10.0	0.1	1.8
K_2O	2.6	0.3	0.8	0.1
MgO	1.0	0.2	0.2	0.1

Table S2 Elemental composition of the **LTA** zeolites determined by ICP analyses.

Sample	Si/Al	Na/Al	Sr/Na
HEU-LTA	1.1	0.9	–
STI-LTA	1.1	0.9	–
Sr-HEU-LTA	1.1	0.14	0.43
Sr-STI-LTA	1.1	0.11	0.45

HEU-LTA-after 4 cycles	1.1	0.5	0.5
STI-LTA-after 4 cycles	1.1	0.7	0.2
Commercial 4A-after 4 cycles	1.1	0.6	0.3

Table S3 Textural properties of HEU-LTA, STI-LTA and commercial 4A.

Sample	Surface area ($m^2 \cdot g^{-1}$) [a]			Pore Volume ($cm^3 \cdot g^{-1}$) [b]		
	S_{BET}	S_{micro}	S_{ext}	V_{total}	V_{micro}	V_{meso}
HEU-LTA	643.1	620.8	22.3	0.29	0.24	0.05
STI-LTA	772.1	755.7	16.4	0.35	0.29	0.06
Commercial 4A	731.9	718.3	13.6	0.29	0.27	0.02

a. Surface area was calculated by BET method.

b. Micropore volumes were determined by t-plot method.

Table S4 Production costs of HEU-LTA, STI-LTA, and commercial 4A calculated based on market prices of the chemicals and raw materials.

Costs (USD/t)	HEU-LTA	STI-LTA	Commercial 4A
NaOH	107	110	108
Sodium aluminate	550	480	496
sodium metasilicate	—	—	319
Total cost	657	590	923

Table S5 Composite building units (CBUs), secondary building units (SBUs), and ring building units (RBUs) of zeolite LTA, HEU, and STI (identical RBUs shared between LTA and HEU or STI are shown in bold).[6-8]

Framework type	CBUs	SBUs	RBUs
LTA	*d4r, sod, lta*	8 or 4-4 or 6-2 or 6 or 1-4-1 or 4	**8**, **6** and **4**
HEU	*bre*	4-4=1	10, **8**, 5 and **4**
STI	*bre, sti*	4-4=1	10, **8**, **6**, 5 and **4**

Table S6 Kinetic parameters of Sr^{2+} adsorption on HEU-LTA and STI-LTA.

Sample	Pseudo-first-order model			Pseudo-second-order model		
	R^2	Q_e (mg·g^{-1})	K_1 (min^{-1})	R^2	Q_e (mg·g^{-1})	K_2 (g·mg^{-1}·min^{-1})
HEU-LTA	0.985	0.192	0.033	0.999	114.94	0.22
STI-LTA	0.924	15.51	0.088	0.999	126.1	0.028

Table S7 Langmuir and Freundlich isotherm parameters of Sr^{2+} adsorption on HEU-LTA and STI-LTA.

Groups	Langmuir isotherm			Freundlich isotherm		
	R^2	Q_m(mg·g^{-1})	K_L(L·mg^{-1})	R^2	n	K_F(mg$^{1-1/n}$·L$^{1/n}$·g^{-1})
HEU-LTA-25°C	0.999	261.8	0.49	0.801	4.71	98.35
HEU-LTA-60°C	0.999	270.3	0.42	0.826	4.66	100.06
HEU-LTA-80°C	0.999	271.0	0.80	0.906	6.03	128.98
STI-LTA-25°C	0.999	308.6	0.82	0.656	4.61	120.48
STI-LTA-60°C	0.992	311.5	0.34	0.810	5.61	131.42
STI-LTA-80°C	0.995	316.5	0.36	0.763	4.52	114.29

a. Determined by ICP analyses.

Table S8 Theoretical maximum adsorption capacities calculated from XRF data.

Sample	Theoretical Q_m (mg·g^{-1})
HEU-LTA	304.53
STI-LTA	338.73

Table S9 The maximum values of distribution coefficient K_d (mL·g^{-1}) of Sr^{2+} by HEU-LTA, STI-LTA and 4A.

Sample	Distribution coefficient (K_d, mL·g^{-1})
HEU-LTA	4.6×10^6
STI-LTA	2.9×10^6

3. References

1. S. Lagergren, About the Theory of So-Called Adsorption of Soluble Substances, *Sven. Vetenskapsakad. Handingarl*, 1898, **24**, 1-39.
2. Y. S. Ho and G. McKay, Pseudo-second order model for sorption processes, *Process Biochem.*, 1999, **34**, 451-465.
3. F. Malatesta, The study of bimolecular reactions under non-pseudo-first order conditions, *Biophys. Chem.*, 2005, **116**, 251-256.
4. I. Langmuir, The adsorption of gases on plane surfaces of glass, mica and platinum, *J. Am. Chem. Soc.*, 1918, **40**, 1361-1403.
5. H. Freundlich, Über die Adsorption in Lösungen, *Z. Phys. Chem.*, 1907, **57U**, 385-470.
6. C. Baerlocher and L. B. McCusker, Database of Zeolite Structures, http://www.iza-structure.org/databases/, (accessed April, 2026.)
7. R. C. F. de Lima, D. d. S. Oliveira and S. B. C. Pergher, Interzeolitic Transformation of Clinoptilolite into GIS and LTA Zeolite, *Minerals*, 2021, **11**, 1313.
8. D. Suhendar, Buchari, R. R. Mukti and Ismunandar, Simple approach in understanding interzeolite transformations using ring building units, *IOP Conf. Ser.: Mater. Sci. Eng.*, 2018, **349**, 012016.